Properties of an Endogenous Steady Current in Rat Muscle

J. H. CALDWELL and W. J. BETZ

From the Department of Molecular and Cellular Biology, National Jewish Hospital and Research Center, and the Department of Physiology, University of Colorado Medical School, Denver, Colorado 80262

ABSTRACT A vibrating probe was used to study a steady electric current generated by isolated, whole lumbrical muscles of the rat. Spatial mapping showed that current leaves the muscle in the synaptic region and re-enters in the flanking extrajunctional regions. The point of maximum outward current coincided precisely with the endplate region. As the probe was moved radially away from the endplate region, the current declined monotonically, and the results could be fit with a simple model. As the probe was moved axially away from the endplate region, the current declined and became inward over a distance of ~0.5 mm. The physiological mechanism by which the current is generated was also studied. α-Bungarotoxin and tetrodotoxin had no significant effect on the current, which suggests that acetylcholine channels and gated sodium channels are not involved in the generation of the current. Ouabain produced a slowly developing, partial inhibition of the current, reducing it by ~40% over a period of 30–40 min. Carbachol produced a large inward current at the endplate region. After the carbachol action was terminated with α-bungarotoxin, an outward current reappeared, and a transient "overshoot" developed. During the overshoot, which lasted ~30–40 min, the outward current was approximately doubled. This overshoot was completely abolished by ouabain. The overshoot is interpreted as reflecting the increased activity of electrogenic sodium pumping in the endplate region, caused by the influx of Na ions during carbachol application. Because of the very different actions of ouabain on the normal current and on the overshoot after carbachol application, we concluded that the normal outward current is not produced by electrogenic sodium pumping in the endplate region.

INTRODUCTION

Skeletal muscle fibers incorporate a number of different membrane pathways to control the movement of ions between the intracellular and extracellular fluids. Some of these pathways are unevenly distributed in the membrane. For instance, certain conductances are partitioned unevenly between the surface and transverse tubular (T) membranes in frog and rat muscle (see Almers et al., 1982, for references). A related question, about which less is known, concerns the distribution of transport pathways along the length of muscle fibers. The pathway best known to be distributed nonuniformly in this respect is the acetylcholine

J. GEN. PHYSIOL. © The Rockefeller University Press · 0022-1295/84/02/0157/17 $1.00

Volume 83 February 1984 157–173

(ACh)-gated channel, whose distribution is normally restricted to the synaptic region (Kuffler, 1943). In addition, inward rectification is stronger at frog muscle endplates than in extrajunctional regions (Katz and Miledi, 1982), and it has been suggested that voltage-sensitive sodium channels are also concentrated near the synapse (Nastuk and Alexander, 1973; Thesleff et al., 1974; Yoshioka, 1981).

A nonuniform spatial distribution of any electrical pathway could lead to steady current flow between different regions of a muscle fiber. This paper describes experiments in which we identified and began to characterize such a current in isolated, whole lumbrical muscles of the rat. The current was measured with a vibrating microelectrode, or vibrating probe (Jaffe and Nuccitelli, 1974; Betz and Caldwell, 1984). We observed a steady outward current at the midregion of the muscle, with flanking regions of inward current. The results suggest that the current is generated by the muscle fibers themselves (and not, for instance, by nerve terminals or Schwann cells), and that the point of maximum outward current coincides with the endplate.

The identity of the ions that carry the current and the pathway(s) by which they cross the membrane were also explored and the results have ruled out several candidate mechanisms. Evidence suggests that ACh channels and voltage-gated sodium channels are not involved in the generation of the current, and also that the outward current is not produced by increased electrogenic Na^+ pumping in the endplate region. A preliminary account of some of this work appeared earlier (Betz et al., 1980).

METHODS

The techniques of construction and calibration of the vibrating probe were the same as described in the preceding paper (Betz and Caldwell, 1984). The biological preparation consisted of the fourth deep lumbrical muscle of the rat (Betz et al., 1979). The tendons were attached to raised platforms in a dish, so that the muscle did not rest on the bottom of the dish. The chamber was elliptical in shape, with perfusion ports located on opposite ends of the chamber. All experiments were performed at room temperature (~25°C). Normal Krebs solution consisted of (mM): 138 NaCl, 5 KCl, 2 $CaCl_2$, 1 $MgCl_2$, 11 glucose, and 2 PIPES (disodium salt) buffer. In a few experiments (results not shown), the pH was buffered with 12 mM $NaHCO_3$ and solutions were bubbled with 95% O_2/5% CO_2; the choice of buffer did not alter the steady outward current.

The output signal of the lock-in amplifier was recorded on a chart recorder. After the experiment, the results were digitized and further analyzed with a Hewlett-Packard (Palo Alto, CA) digitizer and computer. The same computer was used for theoretical calculations.

RESULTS

Spatial Mapping of the Steady Current

Fig. 1*A* shows a typical recording obtained by moving the vibrating probe along the lateral margin of a muscle from one tendon to the other (the probe was vibrated perpendicular to the muscle axis). Current was outward (above baseline) near the middle of the muscle and inward in the flanking regions. Five typical spatial maps are shown in Fig. 1*B*. This "scanning" maneuver was performed at

the outset of each experiment in order to locate the site of maximum outward current. Usually this position could be predicted from the observed pattern of intramuscular nerve branches, the branch closest to the edge being the site of maximum outward current. This was confirmed in some experiments by staining the endplates for ACh esterase. This suggests that the outward current is generated at the synaptic region by cells located close to the edge of the muscle. Moreover, the current is generated by the muscle fibers themselves, since it can be recorded from isolated muscle fibers (Betz et al., 1980) and from denervated muscles (G. L. Harris, unpublished observations).

TWO-DIMENSIONAL MAPPING The procedure described above measured only the component of current that flowed perpendicular to the muscle axis. To construct a two-dimensional map, we measured currents with the probe vibration oriented first perpendicular and then parallel to the muscle axis. Measurements were made at 125-μm intervals, covering a grid ~3 mm (axial) × 0.65 mm (radial) in extent. All measurements were made in the horizontal plane. Then the procedure was repeated with the probe orientation changed by 90°. Results are shown in Fig. 2. In *A* and *B* the amplitude of the recorded signal is plotted against distance along the length of the muscle.

Probe orientation is shown in the insets. The various curves were obtained at different radial positions (the radial distance, in micrometers, is marked on each curve). The zero position was taken as the point at which the maximum outward current was recorded (i.e., the top point in Fig. 2*A*).

In Fig. 2*C* the top traces in *A* and *B* are replotted. According to the one-dimensional cable theory, the membrane current (filled symbols) should be proportional to the first derivative of longitudinal current (open symbols); inspection shows that this is approximated reasonably well. Fig. 2*D* shows the vector sum of the paired recordings at each point; the arrows show the magnitude (proportional to the length of each arrow) and the direction of current recorded at each point.

The radial decay of outward current is shown in Fig. 3. The points were obtained at zero axial distance (i.e., at the position of maximum outward current), with the probe vibration oriented perpendicular to the muscle. The line fitting the points is drawn according to a multiple-quadrupole model described in the previous paper (Betz and Caldwell, 1984). The current density is, from Ohm's law:

$$\vec{i} = \vec{E}/\rho,$$

where ρ is the specific resistivity of the medium and the electric field E is the gradient of the voltage.

$$\vec{E} = -\vec{\nabla} V.$$

For a single quadrupole with the axial distance set equal to zero, the current density as a function of radial distance (y) is given by:

$$i_{\text{radial}} = -\frac{1}{\rho}\frac{\partial V}{\partial y}\bigg|_{x=0} = -\frac{I_d}{2\pi}\left[\frac{y}{(d^2 + y^2)^{1.5}} - \frac{1}{y^2}\right],$$

where d is the distance from the point source (at $x = 0$) to each point sink and I_d is the current entering each point sink ($2I_d$ leaves the point source). The total current at any radial distance was obtained by summing the contributions from a series of quadrupoles with all point sources at $x = 0$ and the point sinks at

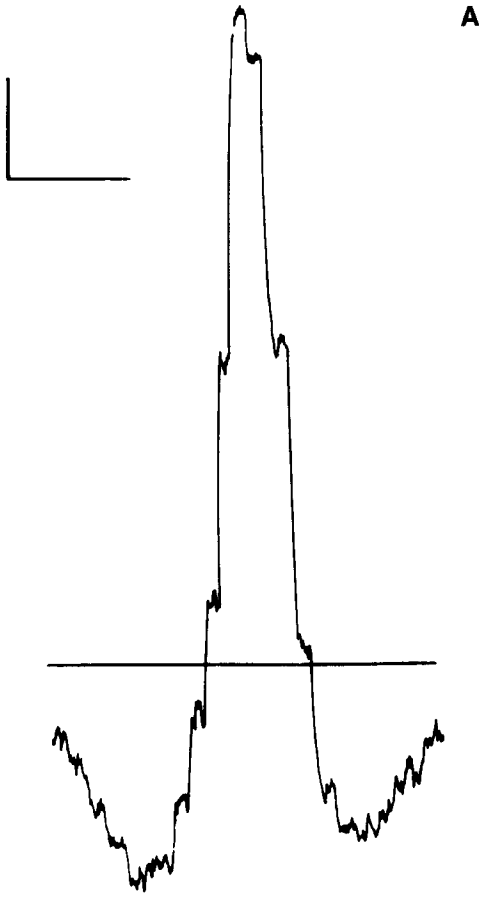

FIGURE 1. Endogenous steady current recorded with the vibrating probe. (*A*) Tracing of the continuous vibrating probe output as the probe "scanned" the edge of the muscle. The probe was first positioned close to the muscle, away from the endplate region (vibration was perpendicular to the muscle axis). About every 20 s the probe was moved in successive steps ~200 μm along the edge of the muscle. The current progressively changed from inward (below the reference line, which was obtained with the probe positioned several millimeters from the muscle) to outward and back to inward as the probe was moved. The total length of the muscle was ~10 mm, and individual muscle fibers run almost from end to end. Calibration marks: vertical = 1.0 μA/cm^2; horizontal = 3 min. (*B*) Maps of recorded current (y axis) against distance along the muscle edge (zero distance = point of maximum outward current). Filled squares show data from *A*. Outward current is positive.

intervals of 20 μm, extending to 3 mm on either side of the point source. To simulate the current flow pattern in a cable, I_d was assumed to decay exponentially with distance from the current source with a length constant of 0.5 mm, which is typical of rat muscle (cf. Betz and Caldwell, 1984). The calculated decay of the current with radial distance cannot be fit by a single power function. Rather, at large distances, the current decays as the inverse fourth power of radial distance, but at positions closer to the muscle, the exponent is closer to zero (cf. Plonsey, 1974).

The data in Fig. 3 could not be fit well by this model using a single scaling factor; the predicted fall-off was steeper than that observed. The line in Fig. 3 was drawn with a further modification: 0.15 mm was added to each radial distance in the model. This additional change is equivalent to assuming that the "real" source of current in the muscle was 0.15 mm deep to the edge of the muscle (since the edge of the muscle was taken as zero distance in the experiment). The actual interpretation is probably more complex than this, since many muscle fibers, located at different distances from the edge of the muscle and with endplates lying in imperfect register, contribute to the current. Given these uncertainties, the fit of the line seems reasonable.

In summary, it is evident from these experiments that rat muscle fibers are surrounded by a current that leaves at the synaptic region and re-enters via the flanking extrajunctional membrane. An electric field is associated with this current and this field is focused at the synapse. Thus, each muscle fiber is embedded in an electric field generated by itself and its neighbors. The polarity of the field is such that in the extracellular fluid the synaptic region behaves as an anode, whereas the neighboring regions are cathodal. Since these experiments were performed on whole muscles, the precise boundary between anodal and cathodal regions remains to be determined.

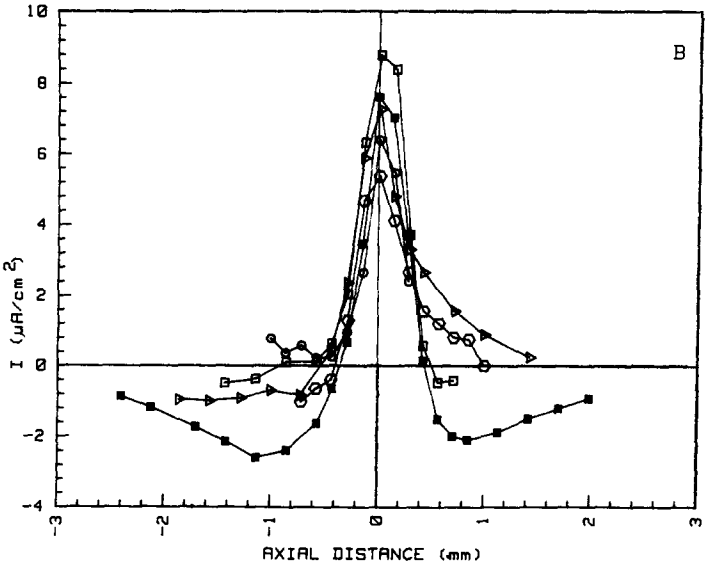

FIGURE 1*B*.

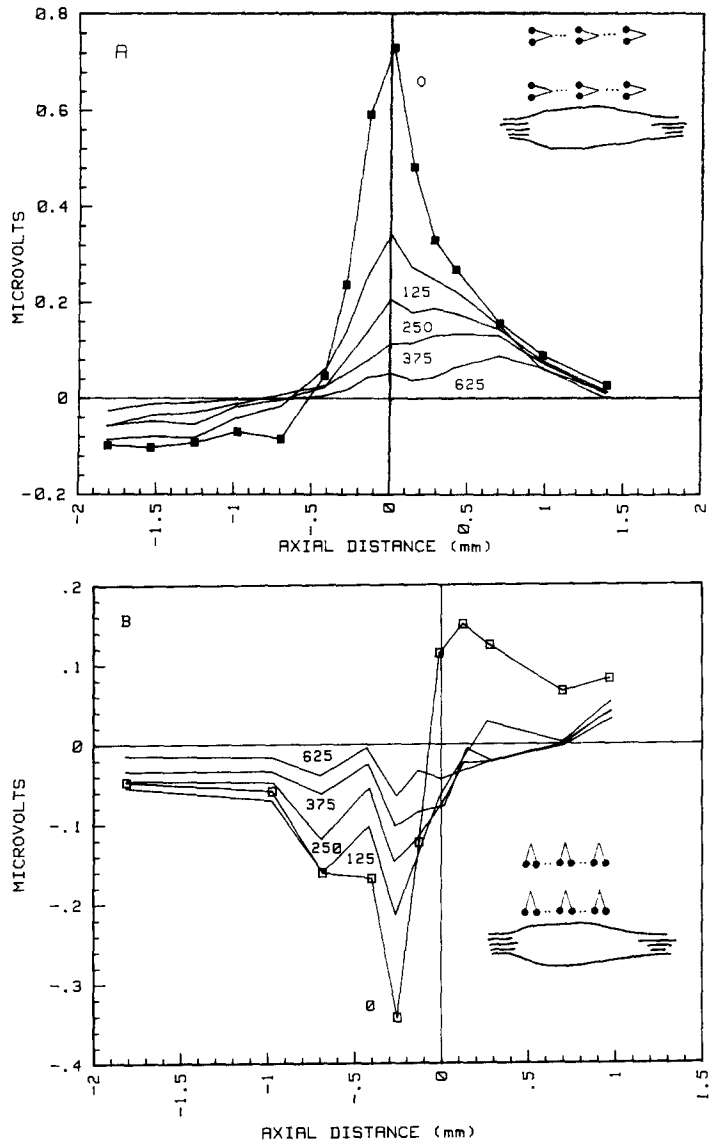

FIGURE 2. Mapping of current in two dimensions. Current measurements were made at different positions near a muscle, all in the horizontal plane. At each position, current was measured with the probe vibrating perpendicular and then parallel to the muscle axis. (*A*) Perpendicular vibration (see inset diagram). The radial distance (i.e., the distance from edge of muscle to probe, in micrometers) is noted on each curve. Zero axial distance on the *x* axis was taken as point of maximum outward current. (*B*) Same as *A*, but probe vibration was parallel to muscle axis. (*C*) Top traces from *A* and *B* are replotted together. Perpendicular vibration (filled symbols) approximates the first derivative of parallel vibration (open symbols). (*D*) Summary diagram showing current magnitude (proportional to length of arrows; calibration lines = 2 $\mu A/cm^2$) and current direction for different radial distances (*y* axis) and different axial distances (*x* axis).

Physiological Mechanism of the Endogenous Current

ACH CHANNELS AND NA CHANNELS Since ACh channels and possibly Na^+ channels (Thesleff et al., 1974) are localized to the synaptic region, it was of interest to determine whether they are involved in the generation of the outward current. Of course, fluxes through these channels produce inward, not outward, current, which means that they could be involved only indirectly in the generation of the endogenous outward current. We tested this possibility by blocking these channels and then measuring the endogenous current over a period of up to 12 h. Fig. 4 shows that α-bungarotoxin had no significant effect on the steady

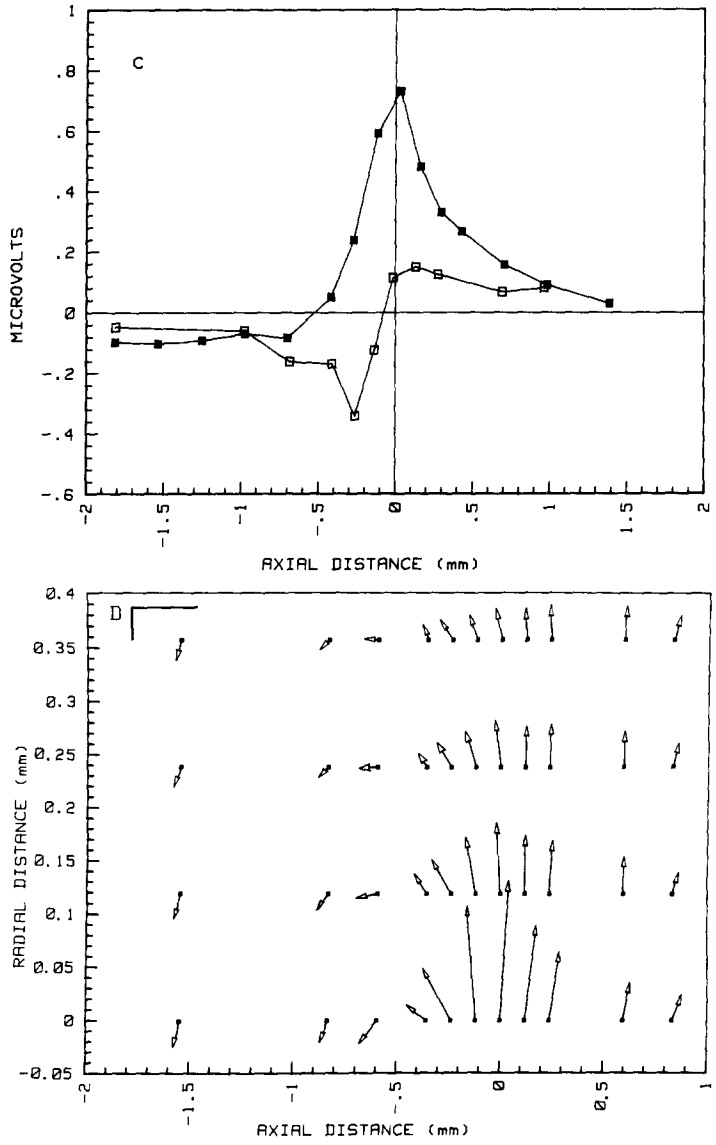

FIGURES 2*C* AND 2*D*.

current. Control experiments showed that the drug totally blocked ACh receptors: subsequent application of carbachol, which produced large inward currents in the absence of α-bungarotoxin, produced no change in the outward current. Similar results were obtained in experiments in which tetrodotoxin (TTX; 3 μM) was added to the bathing solution in order to block Na^+ channels. These experiments, plus others described below, make it unlikely that the steady outward current depends on fluxes through ACh channels or Na^+ channels, at least over a period of many hours.

THE ROLE OF ELECTROGENIC NA^+ PUMPING Another plausible hypothesis is that the outward current reflects increased activity of an electrogenic Na^+ pump in the endplate region (with "extra" Na^+ gaining entry by a route insensitive to α-bungarotoxin and TTX). While preliminary results were consistent with this idea (Betz et al., 1980), further experiments showed that the hypothesis is

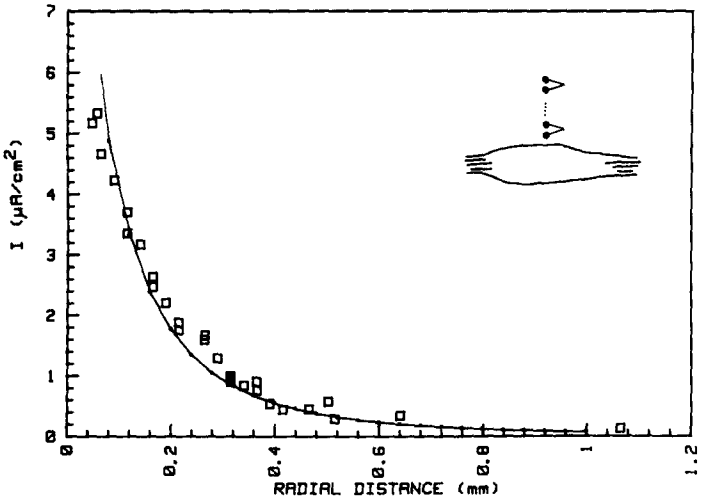

FIGURE 3. Decay of the steady outward current with distance from the edge of the muscle. The axial position was the point of maximum outward current. The line fitting the points was drawn according to a model (see text).

untenable. One prediction of this hypothesis is that ouabain should rapidly abolish the outward current. Typical results from four such experiments are shown in Fig. 5.

Application of 10 mM ouabain at zero time produced a slow inhibition in the outward current; the current declined by ~40% over a 30–40-min period. The slow inhibition probably reflects a general run-down of ion electrochemical gradients and suggests that the normal outward current is not produced by electrogenic sodium pumping.

This conclusion is somewhat equivocal, however, since it has been suggested that rat muscle is relatively resistant to the blocking effects of ouabain (Detwiler, 1967). Thus, a different series of experiments was performed in order to test further the electrogenic pump hypothesis. The following experiments show that electrogenic Na^+ pumping could be selectively stimulated in the endplate region,

but that the effects of ouabain and other agents on this electrogenic current were very different from their effects on the endogenous outward current.

Fig. 6 shows the effect of bath-applied carbachol on the steady current. At zero time, the recording chamber was perfused with a solution containing

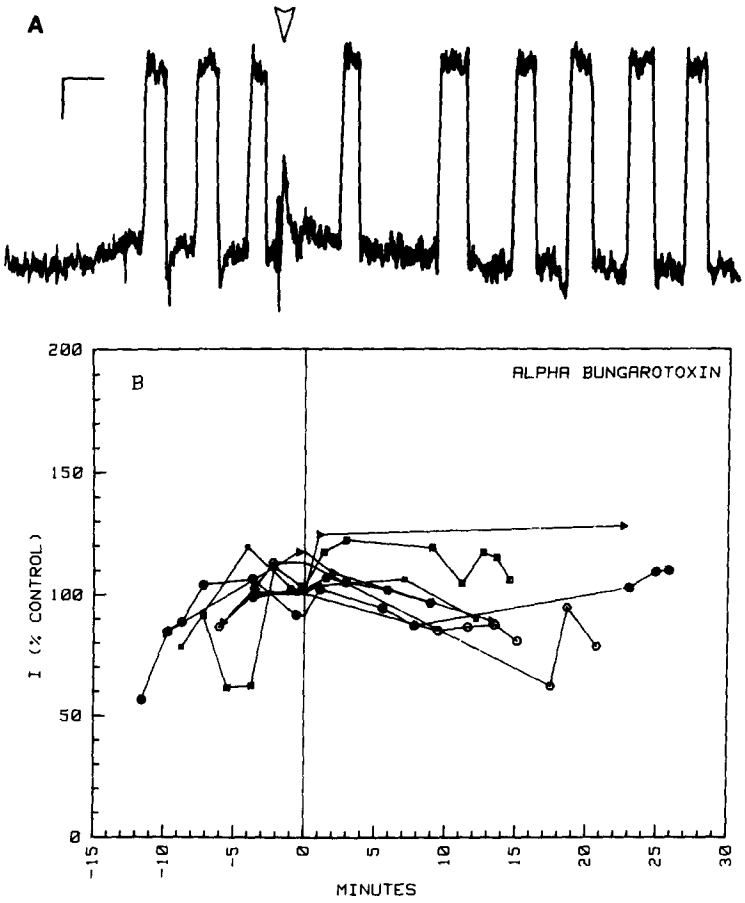

FIGURE 4. Effect of α-bungarotoxin on the steady outward current. (*A*) Chart recording of the probe signal at position of maximum outward current. The probe was moved alternately between a remote reference position (baseline signal) and a position adjacent to the muscle. α-Bungarotoxin (4 μg/ml) was added at time marked by arrow. Calibration: vertical = 1 μA/cm^2; horizontal = 1 min. (*B*) Superimposed records from eight experiments. Toxin was added at zero time. For each experiment the probe signal is normalized to the pre-toxin level.

carbachol (165 μM). The current immediately became large and inward. Then, at the time marked by the arrow, the chamber was perfused with normal Krebs containing curare (13 μM) in order to arrest the carbachol action. The current then became outward, and an overshoot developed. The overshoot can be seen more clearly in the inset, where the large inward current is not plotted.

It is likely that the overshoot following carbachol treatment was produced by electrogenic Na^+ pumping in the endplate region, stimulated by the carbachol-induced influx of Na^+. Results from other experiments are consistent with this explanation. For instance, the overshoot was greatly reduced when external Na^+ was replaced by Li^+ (Fig. 7*A*), and Li^+ is known to be a poor substitute for Na^+ in the Na^+ pump (Keynes and Swan, 1959). It was also of interest to test the effect of Cl^- substitution on the overshoot, because (as described in the following paper) removal of external Cl^- abolishes the steady outward current. Cl^- substitution should not, however, have much effect on electrogenic Na^+ pumping, and this in fact was observed (Fig. 7*B*).

The best evidence that the overshoot was produced by electrogenic Na^+ pumping in the endplate region was obtained in experiments with ouabain. This

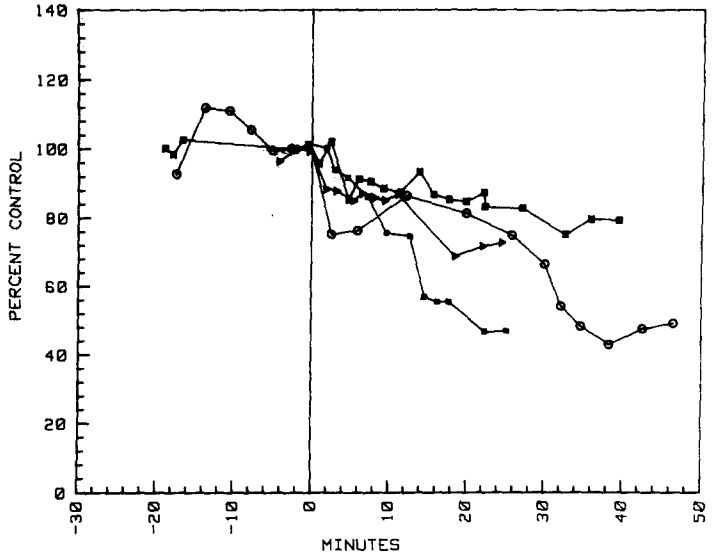

FIGURE 5. Effect of ouabain on the steady current. Normal Krebs containing 10 mM ouabain was added at zero time; responses are normalized to the pre-toxin level.

drug completely blocked the post-carbachol overshoot, as shown in Fig. 8. Filled symbols show the large overshoots observed in control muscles (no ouabain). In the other experiments, ouabain was added several minutes before the addition of carbachol and was present for the rest of the experiment. Carbachol was present for up to 10 min, and at zero time normal Krebs containing α-bungarotoxin (4 μg/ml) was introduced. Large inward currents in carbachol were observed in all cases; these are not plotted. Ouabain completely blocked the overshoot at concentrations of 10 (open circles) and 100 μM (open squares). It was less effective at 1 μM (dots). These results provide further evidence that the current overshoot is produced by electrogenic Na^+ pumping in the endplate region. It is clear that the action of ouabain on the post-carbachol overshoot is very different from its action on the steady outward current.

Fig. 9 shows spatial maps obtained in normal Krebs (triangles) and in the presence of carbachol (squares). The point of maximum outward current in normal Krebs corresponds exactly to the point of maximum inward current in carbachol, which provides further evidence that the endogenous outward current is generated at the synaptic region.

EFFECTS OF CHANGES IN EXTERNAL [CA^{++}] Fig. 10 shows the effects of removal of external Ca^{++}. During the time marked by the heavy line, bathing solutions contained 1 mM EGTA and no added Ca^{++}. The normal outward current, the inward current in carbachol, and the post-carbachol overshoot were not significantly affected by Ca^{++} removal. Similarly, high (10 mM) Ca^{++} did not affect the steady outward current.

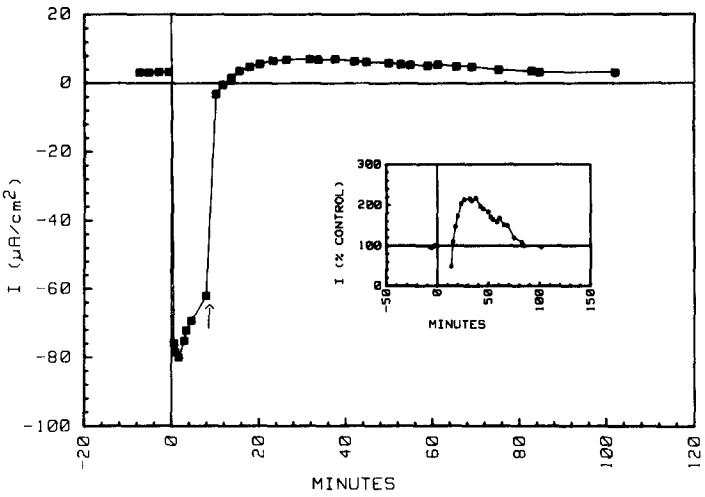

FIGURE 6. Effect of carbachol on the endogenous current. Normal Krebs containing carbachol (165 μM) was added at zero time. At the time marked by the arrow, the carbachol solution was replaced by normal Krebs containing curare (13 μM). Inset: outward currents are replotted to show the distinct overshoot that followed the washout of carbachol. Currents are normalized to pre-carbachol level.

Measurements of Resting Potential

A steady outward current generated in the endplate region should hyperpolarize the muscle fiber at that site. We estimated that the total outward current generated by isolated muscle fibers was ~1 nA (Betz et al., 1980). In a typical rat muscle fiber, this should produce a hyperpolarization at the endplate of a few tenths of a millivolt. The amount of hyperpolarization should be increased several-fold after carbachol treatment.

We recorded membrane potentials at endplates and in extrajunctional regions both before and after carbachol treatment. The results are given in Table I. After carbachol treatment, endplates were clearly hyperpolarized, relative to extrajunctional regions, by a few millivolts. In control muscles, however, no significant difference was observed. This probably reflects the relatively large

standard deviation of normal resting potentials (~3–4 mV). It is possible to estimate the approximate number of samples needed to reach a particular P value, assuming two populations with the same standard deviation and different means (Snedecor and Cochran, 1980). For the case at hand, in order to be 90% certain of reaching the 5% confidence level, ~800 impalements would be necessary. Thus, it is not surprising that the data in Table I from normal muscles are not significantly different, given the limited sample size. Using a larger sample size than in our study, Yoshioka and Miyata (1983) reported that resting potentials in the endplate region of rat soleus muscle are significantly more

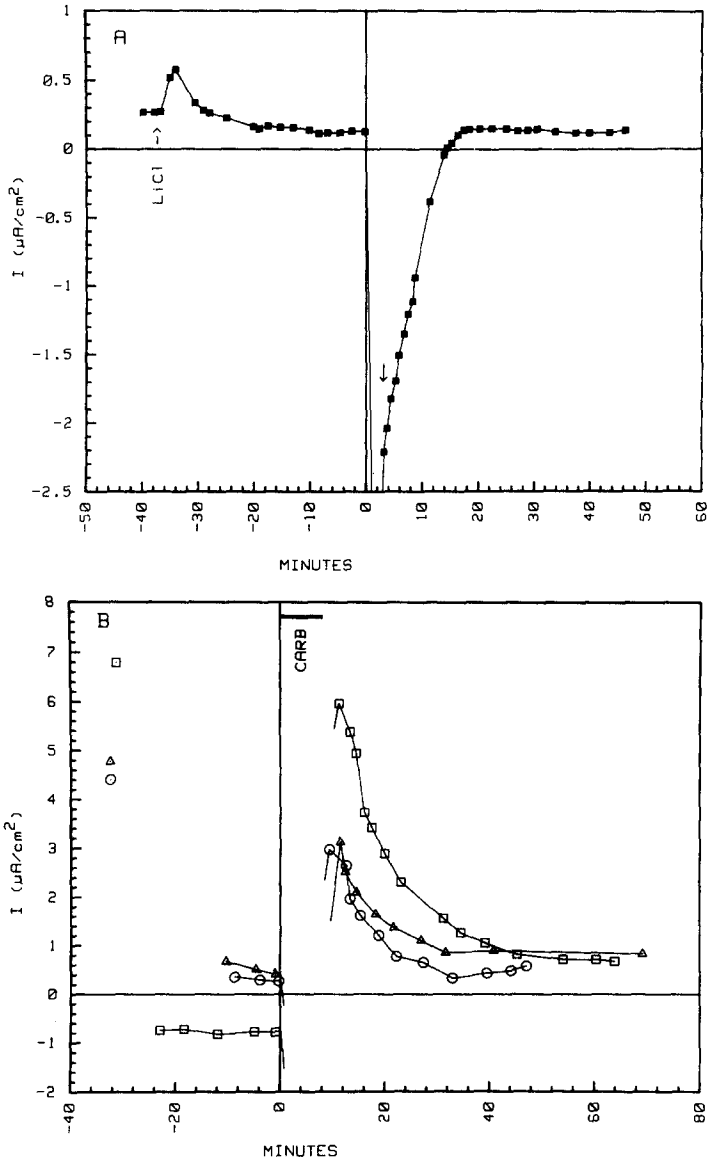

FIGURE 7.

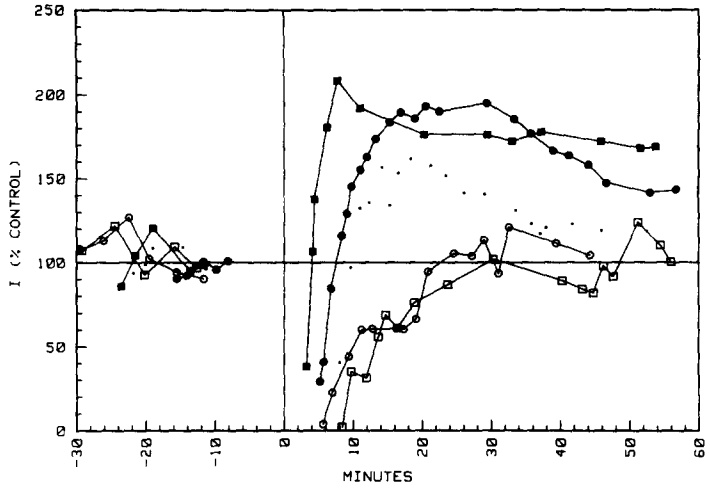

FIGURE 8. Effect of ouabain on the overshoot after carbachol treatment. Responses normalized to pre-carbachol levels. Filled symbols show overshoots in normal Krebs (no ouabain). Zero time represents the time at which carbachol was washed out (it was present for 5–10 min, and in every case it produced a large inward current, which is not shown). In three experiments, ouabain was added 10–15 min before zero time and was present for the rest of the experiment. Ouabain concentrations: open squares = 100 μM; open circles = 10 μM; dots = 1 μM. Ouabain reduced or abolished the outward current overshoot.

negative (by ~1 mV) than in extrajunctional regions. Rat soleus muscle also generates a steady outward current in the endplate region (our unpublished observations).

DISCUSSION

Spatial Properties of the Endogenous Current

Although it seems clear that the point of maximum outward current coincides with the endplate, the precise boundary between outward and inward current-

---

FIGURE 7 (*opposite*). Effect of Na^+ and Cl^- replacement on the response to carbachol. (*A*) At the time marked by the first arrow, Na^+ was replaced by Li^+. At zero time, the same solution containing carbachol (165 μM) was introduced, and the current became large and inward. At the second arrow, the action of carbachol was terminated with Li^+ Krebs containing α-bungarotoxin (4 μg/ml). The current again became outward, but there was little overshoot. (*B*) Same protocol as *A*, but with Cl^- replacement (Cl^- replaced with isethionate). Results from three experiments. Control levels of outward currents in normal Krebs are shown by the individual symbols at the upper left. Cl^--free Krebs reduced the steady current to the levels indicated just before zero time. Carbachol was present during the time marked by the bar; large inward currents were produced by the carbachol (not shown). At the end of the carbachol treatment, Cl^--free Krebs containing α-bungarotoxin was added, and a large outward current overshoot developed.

generating membrane remains to be established. In experiments on whole muscles, the distance along the edge of a muscle over which outward current could be recorded was typically 0.5–1.0 mm, which is much larger than an individual endplate (~40 μm). The entire endplate band, which encompasses all endplates, is ~0.5 mm wide in rat lumbrical muscle, but only those fibers near the edge appear to contribute to the signal recorded by the probe. The axial dispersion of these edge-fiber endplates is ~100–200 μm, which is several times smaller than the length over which outward current was recorded. This might suggest that the outward current generator in a single fiber extends beyond the endplate margin. However, spatial resolution is affected significantly by the radial distance between the current source and the vibrating probe (see Betz and

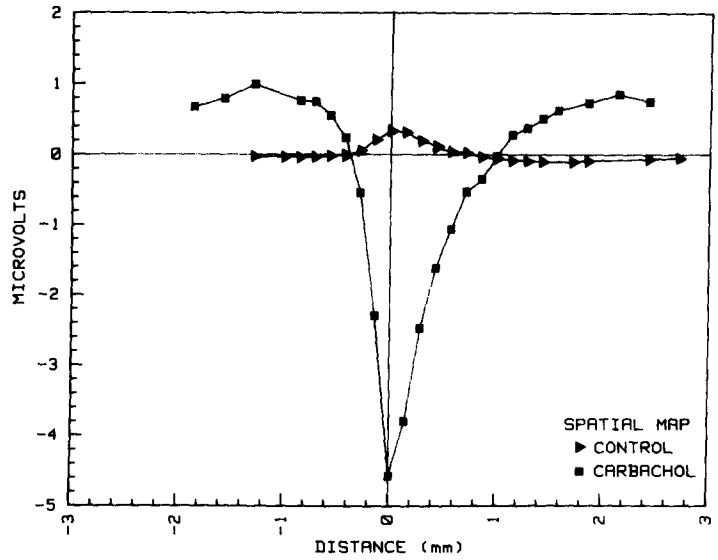

FIGURE 9. Spatial maps of steady currents before (triangles) and during (squares) the action of carbachol. The spatial coincidence of the peaks is evidence that the normal outward current is generated at the synaptic region.

Caldwell, 1984). It is difficult to estimate quantitatively the contribution of this effect, given the somewhat dispersed locations of the endplates. Thus, further experiments will be necessary in order to determine whether the outward current is precisely coincident with the endplate.

Physiological Properties of the Current

α-Bungarotoxin, curare, and TTX had no effect on the steady outward current, which makes it unlikely that fluxes through ACh channels or Na^+ channels are involved in the generation of the current. The current was normal in the absence of HCO_3^-, and the removal of Ca^{++} also had no significant effect on the outward current, which suggests that these ions are not involved in its generation.

Experiments with ouabain suggested that the outward current is not produced

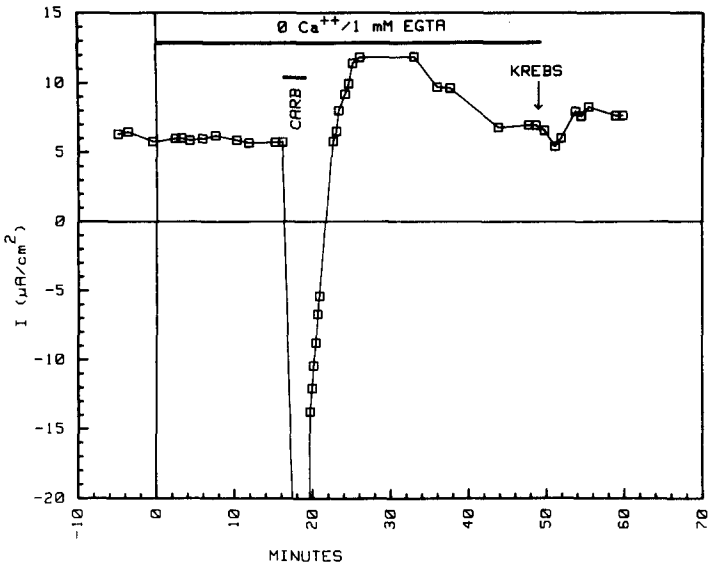

FIGURE 10. Effect of Ca^{++} removal on the endogenous current. Ca^{++}-free Krebs containing 1 mM EGTA was present during the time marked by the heavy line. Carbachol (165 μM) was added at the time shown on the graph, producing a large inward current. α-Bungarotoxin was added when carbachol was removed, and a transient overshoot in the outward current developed. Returning the muscle to normal Krebs (KREBS) had little additional effect. These results are like those obtained in normal Krebs (Fig. 6).

as a result of increased electrogenic Na^+ pumping in the endplate region. Ouabain at high concentration (10 mM) produced a relatively small, slowly developing inhibition of the outward current (Fig. 5). By contrast, it more rapidly and completely abolished another current, which itself was probably due to electrogenic Na^+ pumping at the endplate region. This current was stimulated by loading the muscle fibers with Na^+ in the endplate region: the Na^+ entered through ACh channels opened by bath-applied carbachol. When the carbachol action was terminated, a large outward current (overshoot) developed, which declined over a period of 30–60 min to control levels. Ouabain (10 μM) totally

TABLE I

Position and treatment	Mean RMP	SD	*N*
	mV	*mV*	
(1) Endplate, normal	−76.7	4.24	68
(2) Endplate, carbachol	−78.3	3.43	55
(3) Extrajunctional, normal	−76.1	3.55	52
(4) Extrajunctional, carbachol	−75.7	3.41	52

Resting membrane potentials (RMP's) were recorded at different positions (endplate or extrajunctional region) under different conditions (in normal Ringer or after carbachol treatment). Results of *t* tests are: 1 vs. 2: $P = 0.01$; 3 vs. 4: $P = 0.48$; 2 vs. 3 and 4: $P = 0.001$.

inhibited this overshoot. Since the actions of ouabain on the normal steady current and on the apparent electrogenic Na^+ pump were very different, it seems reasonable to conclude that the normal outward current is not produced by electrogenic Na^+ pumping. Of course, this conclusion should not be taken to suggest that Na^+ pumps in rat lumbrical muscle are not electrogenic. Uniformly distributed electrogenic Na^+ pump sites would produce current loops on a submicron scale, which would not be detectable by the vibrating probe.

Thus, the physiological basis of the outward current remains to be determined. Other models, in which the conductance to different ions differs at endplate and extrajunctional regions, are tested in the following paper.

We thank Drs. David Gadsby and Paul De Weer for advice and suggestions, and Tom Evans and Mark Lupa for technical assistance in the course of the experiments.
This research was supported by National Institutes of Health grants NS 16922 (to J.H.C.) and NS 10207 (to W.J.B.) and by a grant from the Muscular Dystrophy Association of America (to W.J.B.).

Received for publication 6 July 1982 and in revised form 10 August 1983.

REFERENCES

Almers, W., R. Fink, and N. Shepherd. 1982. Lateral distribution of ionic channels in the cell membrane of skeletal muscle. *In* Disorders of the Motor Unit. D. L. Schotland, editor. John Wiley & Sons, New York. 349–366.

Betz, W. J., and J. H. Caldwell. 1984. Mapping electric currents around skeletal muscle with a vibrating probe. *J. Gen. Physiol.* 83:143–156.

Betz, W. J., J. H. Caldwell, and R. R. Ribchester. 1979. The size of motor units during post-natal development of rat lumbrical muscle. *J. Physiol. (Lond.).* 297:463–478.

Betz, W. J., J. H. Caldwell, R. R. Ribchester, K. R. Robinson, and R. F. Stump. 1980. Endogenous electric field in skeletal muscle depends on the Na/K pump. *Nature (Lond.).* 287:235–237.

Detwiler, D. K. 1967. Comparative pharmacology of cardiac glycosides. *Fed. Proc.* 26:1119–1124.

Jaffe, L. F., and R. Nuccitelli. 1974. An ultrasensitive vibrating probe for measuring steady extracellular currents. *J. Cell Biol.* 63:614–628.

Katz, B., and R. Miledi. 1982. An endplate potential due to potassium released by the motor nerve impulse. *Proc. R. Soc. Lond. B Biol. Sci.* 216:497–507.

Keynes, R. D., and R. C. Swan. 1959. The permeability of frog muscle fibres to lithium ions. *J. Physiol. (Lond.).* 147:626–638.

Kuffler, S. W. 1943. Specific excitability of the end plate region in normal and denervated muscle. *J. Neurophysiol.* 6:99–110.

Nastuk, W. L., and J. T. Alexander. 1973. Non-homogeneous electrical activity in single muscle fibers. *Fed. Proc.* 32:333. (Abstr.)

Plonsey, R. 1974. The active fiber in a volume conductor. *IEEE (Inst. Electr. Electron. Eng.) Trans. Biomed. Eng.* 21:371–381.

Snedecor, G. W., and W. G. Cochran. 1980. Statistical Methods. Iowa State University Press, Ames, IA. 102ff.

Thesleff, S., F. Vyskocil, and M. R. Ward. 1974. The action potential in end plate and extrajunctional regions of rat skeletal muscle. *Acta Physiol. Scand.* 91:196–202.

Yoshioka, K. 1981. Effects of cordotomy on the distribution of ACh sensitivity and membrane electrical properties of rat skeletal muscle. *Ochanomizu Igaku Zasshi.* 29:31–41. (in Japanese).

Yoshioka, K., and Y. Miyata. 1983. Changes in the distribution of the extrajunctional acetylcholine sensitivity along muscle fibers during development and following cordotomy in the rat. *Neuroscience.* 9:437–443.